

# Fabrication and characterization of nano-structured ferromagnetic $\text{Ti}_{1-x}\text{Fe}_x\text{O}_2$ thin films

R.Apetrei\*, C.Negrilă\*\*, D.Macovei\*\*, V.Dăscăleanu\*, C.-M.Teodorescu\*\*, D.Mardare\*, D.Luca\*

\*Alexandru Ioan Cuza University, 11 Carol I Blvd. 700506-Iași, Romania, dimitru.luca@uaic.ro

\*\*National Institute of Materials Physics Bucharest

P.O. Box MG-7, 077125 Măgurele-Ilfov Romania, teodorescu@infim.ro

## ABSTRACT

Nanostructured intrinsic and doped titania materials have long been subject to both basic and applied research, in connection with environment and energy-related applications. Apart from beneficial effects, such as widening the wavelength range for surface photocatalytic activation, doping  $\text{TiO}_2$  materials with 3d ferromagnetic cations is a main route to develop an important class of diluted semiconductors, with potential applications in spintronics. In all the previous investigations the concentration of the ferromagnetic dopant was limited to a few percents. Here, we initiate an extended investigation of  $\text{Ti}_{1-x}\text{Fe}_x\text{O}_2$  within a wider iron composition range ( $x = 0 - 0.55$ ) and discuss the magnetic and optical properties of these materials in thin films in relation with their elemental composition, nano-structure and local atomic ordering.

**Keywords:**  $\text{Ti}_{1-x}\text{Fe}_x\text{O}_2$  thin films, optical and magnetic properties, titanium suboxides, magnetite hematite.

## 1 INTRODUCTION

Intrinsic  $\text{TiO}_2$  and doped nano-structured titania materials have benefitted from special interest in materials science for decades, leading to a number of already well-documented applications in environment- and energy-related applications. High efficiency photocatalytic, bactericidal, and super-hydrophilic titania materials based on anatase  $\text{TiO}_2$  are utilized as such, or as a main component in several devices, like gas sensors and dye-sensitized solar cells [1]-[4]. Additionally, diluted magnetic semiconductors prepared by doping titania with small amounts of ferromagnetic impurities (Co, Fe) are now under intensive study, due to promising applications in spintronics. The results reported here are related to this latter research domain, aiming to extend the characterization of these materials towards heavy doping conditions.

We report here on the fabrication of Fe-doped  $\text{TiO}_2$  and the investigation of the relation between their electronic structure and magnetic and optical properties. The current results are correlated with the elemental composition and ionization state, structure and morphology, as well as local atomic ordering.

## 2 EXPERIMENTAL DETAILS

The 200 nm thick film samples have been prepared in an RF magnetron sputtering facility (13.56 MHz,  $2.5 \times 10^{-5}$  mbar base pressure). A constant forward power of 80 W and an Ar discharge pressure of  $5.5 \times 10^{-3}$  mbar were kept unchanged in all the preparation experiments. A 3" ceramic  $\text{TiO}_2$  disk target (K. J. Lesker) was used to grow intrinsic  $\text{TiO}_2$  films, which served as reference samples. To fabricate the heavily Fe-doped films, a mosaic consisting of 1 to 4 sintered pellets of  $\text{Fe}_2\text{O}_3$ , 2 mm in diameter, was placed on the upward-facing  $\text{TiO}_2$  target in the high-rate sputtering area. Microscope glass slides kept at 250 °C during deposition were used as film substrates.

The XPS technique was used to derive the elemental composition and chemical state, by using a PHI Versa Probe 5000, monochromated Al  $K_\alpha$  radiation and 45° take-off angle. All sample measured were calibrated with respect to the C1s peak at 284.6 eV. The structure of the films was investigated by using a XRD diffractometer (Bruker D8, grazing angle) with Cu  $K_\alpha$  radiation. Film surface morphology was investigated from the AFM images using a NT-MDT SolverPro 7M microscope operated in the tapping mode. The band gap values were calculated from transmittance data (Perkin Elmer) using the standard procedure [5]. The magnetic characteristics have been inferred from MOKE loops (AMACC Anderberg & Modéer Accelerator instrument) with the magnetic field lines parallel to film surface.

X-ray absorption fine structure spectroscopy (XAFS) measurements were performed at the Hasylab storage ring facility in Hamburg, Germany, on the beamline E4 (EXAFS II). X-rays produced by a bending magnet were pre-focused by a toroidal mirror (Au or Ni-coated) and then passed through a double-crystal Si(111) monochromator. Fluorescence yield of the Fe-doped titania thin films was measured by recording the  $K_\alpha$  fluorescence of Ti or Fe using a 7-pixel Si(Li) detector, while scanning the excitation photon energy over the corresponding K-edges. The reference samples were metal foils of Fe (thickness: 7  $\mu\text{m}$ ) and Ti (5  $\mu\text{m}$ ), or  $\text{Fe}_2\text{O}_3$ ,  $\text{Fe}_3\text{O}_4$ ,  $\text{TiO}_2$  and TiO powders (about 20 mg) pressed in pellets with cellulose. The reference samples were measured in transmission mode by recording the incident and trans-

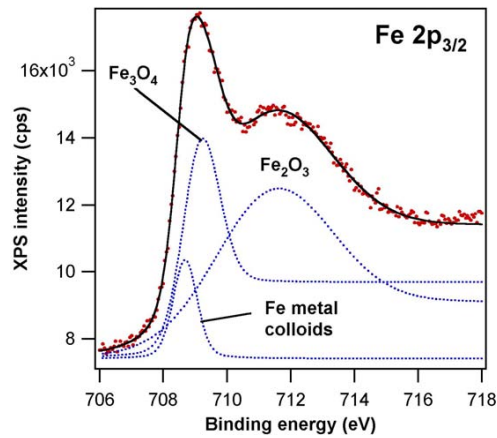


Figure 1: The Fe  $2p_{3/2}$  signal in the XPS spectra of the investigated films

mitted X-ray intensities with ionization chambers.

### 3 RESULTS AND DISCUSSION

The XPS measurements show that the Fe/Ti atomic ratio in the doped samples changes as shown in Table 1. The as-prepared reference samples are oxygen deficient; the O/Ti atomic ratio in the reference sample is 1.79 and is fluctuating around the same value in the doped films. Two components, namely a "bulk" (BE = 532.5 eV) and a "surface" (BE = 533.3 eV) ones are present in the O  $1s$  XPS peak, while the Ti  $2p_{3/2}$  XPS peaks (not shown here) features a main  $\text{TiO}_2$  component, along with  $\text{Ti}_2\text{O}_3$  and other suboxides. As an example, we show in Fig. 1 the  $2p_{3/2}$  Fe peak of the Fe 2/4 sample. In all the Fe-containing samples the Fe  $2p_{3/2}$  peak could be deconvoluted into three components: (i) the  $\text{Fe}^0$  non-reacted component, whose weight diminishes when increasing  $x$  between 0 and 0.55, from 0.33 to 0.1 percent of the total Fe amount; (ii) the  $\text{Fe}^{2+}$  component weighting about 0.15 percent in all the doped samples, and (iii) the  $\text{Fe}^{3+}$  component weighting the balance.

Intensive A(101) and weak A(004) peaks occur in the XRD patterns of Fe 0 reference film, exclusively. Apart from the reference sample, the XRD signals originating in nano-structured domains were below the detection limit of the instrument.

The AFM images showed that the surface roughness diminishes by introduction of Fe in the films. The roughness maximum in the AFM surface histograms occurs at 13 nm in the case of the reference sample, but remains below this value, as shown in Table 1, upon increasing of the Fe content. A  $1\mu\text{m} \times 1\mu\text{m}$  AFM surface view of Fe 1/4 sample is shown in Fig. 2. Small grains occur as spread inside a rather smooth surface.

Fig. 3 depicts the X-ray absorption near-edge spectra (XANES) at the Ti K-edge of the highest Fe-content sample (Fe 4/4) along with the XANES spectra of stan-

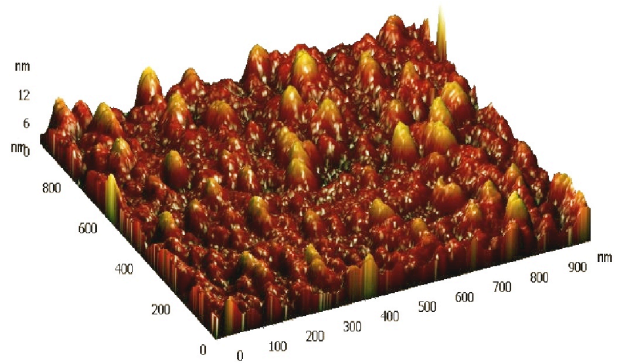


Figure 2: The 3D AFM image of the Fe 1/4 sample.

dard anatase  $\text{TiO}_2$  and of  $\text{TiO}$ , respectively. A first remark concerns the pre-edge peak in the range 4962 - 4972 eV. This peak is a sign of dipole forbidden transitions  $1s \rightarrow 3d$  and may be used to ascertain the number of  $3d$  holes,  $n_h(3d)$ [6]. The calculated amplitude of this pre-edge peak (measured in absorption  $\times$  energy units and weighted by the amplitude of the absorption jump) is 0.625 eV for the case of  $\text{Ti}^{4+}$  [ $\text{TiO}_2$ , with  $n_h(3d) = 10$ ], 0.313 eV for the Fe 4/4 sample, and 0.232 eV for the  $\text{Ti}^{2+}$  case [ $\text{TiO}$ , with  $n_h(3d) = 8$ ]. By plotting the values obtained for  $\text{Ti}^{4+}$  and  $\text{Ti}^{2+}$  vs.  $n_h(3d)$  and taking into account the experimentally proven lack of pre-edge peak in the spectrum of the reference metal (Ti) spectrum [ $n_h(3d) = 7$  for  $4s^1 3d^3$  configuration], one obtains an almost straight line, which may be used to interpolate for the sample Fe 4/4 a number of  $3d$  holes of 8.38 and hence an ionization state of  $2.38+ \approx 2.4+$ .

The XANES data suggest that a titanium suboxide compound with an approximate average stoichiometry of  $\text{Ti}_5\text{O}_6$  (or even  $\text{Ti}_4\text{O}_5$ ) is formed in the films. Suboxide occurrence was also reported in our previous work on reactive pulsed laser deposited titania films [7]. This oxygen depletion might be ascribed to an increased oxygen uptake by iron. This latter process can furthermore lead to the occurrence of iron oxide nanoparticles, as we will discuss later on.

Fig. 4 shows the XANES spectra at the Fe K-edge for all samples. Spectra of metal Fe and of the two most common iron oxides, namely hematite ( $\alpha\text{-Fe}_2\text{O}_3$ ) and magnetite ( $\text{Fe}_3\text{O}_4$ ) are also presented. It is straightfor-

Table 1: Sample main data.

Sample id.	Surface roughness (nm)	Fe/Ti atomic ratio	$E_g$ (eV)
Fe 0	13	0.00	3.27
Fe 1/4	8	0.28	2.85
Fe 2/4	5	0.49	2.50
Fe 3/4	5	0.85	2.27
Fe 4/4	8	1.22	2.21

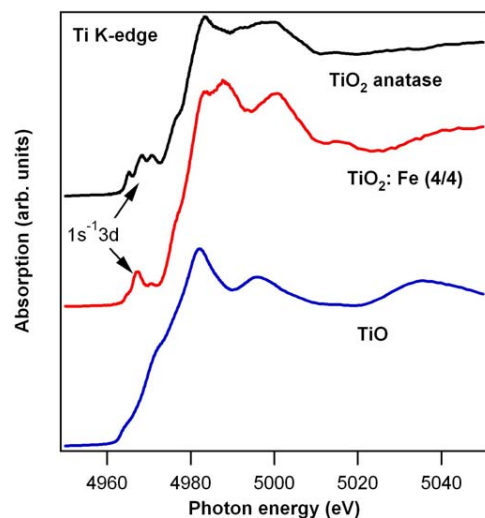


Figure 3: Ti K-edge X-ray absorption near-edge spectra (XANES) of anatase  $\text{TiO}_2$ , of a Fe-doped titania film (sample Fe 4/4), and of TiO.

ward that the XANES spectrum of the sample Fe 4/4 resembles closely the spectrum of magnetite, at least with respect to the presence and relative amplitude of the XANES resonances A, B and D. In addition, the spectra of iron-doped titania samples show an additional XANES resonance, C, which is specific to the XANES spectrum of metal Fe and whose relative amplitude in the spectrum seems to increase when going from Fe 4/4 to Fe 3/4 and to Fe 2/4. Consequently, the Fe K-edge XANES suggest that the sample contains magnetic nanoparticles of magnetite  $\text{Fe}_3\text{O}_4$  and of metal Fe. Nevertheless, the presence of hematite-like particles cannot be completely ruled out.

While the origin of the pre-edge resonance A are in the dipole-forbidden transitions discussed above, the origin of resonance B resides mainly in the  $1s \rightarrow 4p$  transitions [8], whereas peak D is a multiple-scattering resonance in the anionic cage [9]. The peak C from the metal Fe XANES spectrum originates from the van Hove band singularity and may be smoothed out in the case of metal clusters [9]. It is not surprising that Fe tends to form clusters while deposited in titania: a similar behaviour is well known from surface science studies of Fe deposited on InAs [10] or even on GaAs [11].

Fig. 5 shows the moduli of the Fourier transforms of  $k^2$ -weighted EXAFS function  $\chi(k)$ , where  $k$  is the photoelectron wavevector, and  $\chi = \Delta\mu/\mu_0$  the relative oscillations of the absorption spectrum above the Fe K-edge. These Fourier transforms are roughly proportional to the radial distribution function (RDF) around the absorbing atoms (Fe in this case) [12]. Here the results contradict somehow the XANES observations: (i) the first maximum in the RDF of the iron-doped titania samples does not resemble the corresponding region in

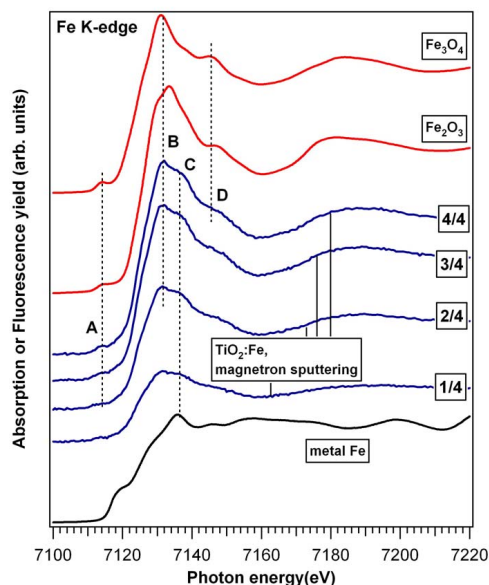


Figure 4: Fe K-edge X-ray absorption near-edge spectra (XANES) of reference magnetite ( $\text{Fe}_3\text{O}_4$ ), hematite ( $\text{Fe}_2\text{O}_3$ ), Fe-doped titania films, and Fe metal. For discussions on the resonances A-D, see the text.

any of the standard oxides, nor in the metal sample; (ii) the sample Fe 4/4 features a second RDF maximum which resembles that of hematite and only the sample Fe 3/4 (and partly Fe 2/4) has a second maximum closer to magnetite; (iii) the samples do not feature the specific maxima of the RDF of metal Fe; the sample Fe 3/4 shows a wide 3-rd maximum located close the Fe metal third coordination shell. A discrepancy results between the Fe K-edge XANES and EXAFS, most obvious in the Fe 4/4 spectra, i.e the Fe XANES spectrum suggests the co-existence of magnetite and metal Fe; the EXAFS spectrum at the same edge shows a second maximum in the Fourier transform, quite similar to the one in the hematite spectrum. This issue requires further analysis, we may only state for now that the XANES spectrum depends mainly on the nearest-neighbor configuration, whereas when discussing the second maximum in the Fourier transforms we refer to the second coordination shell, with possible insertion of some Ti cations. This second shell may be distorted such as to resemble the second coordination shell of *hematite*.

The hysteresis loops of the ferromagnetic samples measured using the MOKE technique is shown in Fig. 6. An increase of the magnetization by a factor of six can be observed under a magnetic field intensity of 31.6 kA/m for the highest iron content film. A monotonous increase of the maximal Kerr rotation angle with the increase of the iron content in the samples is demonstrated. Additionally, the maximum-field intensity values available in our MOKE experiment did not allow us to approach the saturation conditions, mainly for the

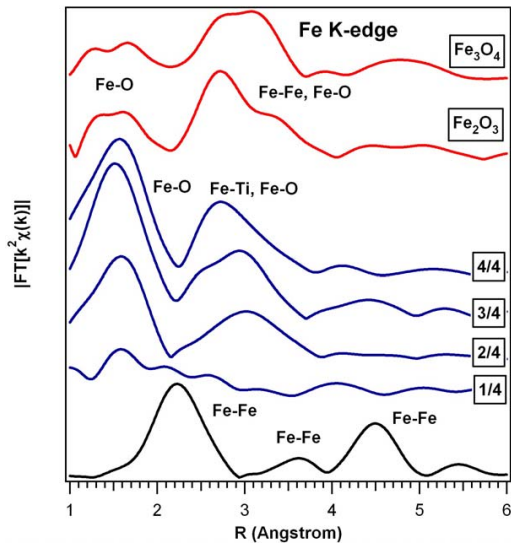


Figure 5: Fourier transforms of the Fe K-edge EXAFS functions of magnetite, hematite, Fe-doped titania, and Fe metal; the EXAFS functions are weighted by the square of the photoelectron wavevector  $k^2$ .

high iron content samples. No detectable MOKE signal was registered with the pure  $\text{TiO}_2$  films.

The oxygen-depletion and the consequent occurrence of titania suboxides result in  $n$ -doped films [3]. The effect of increasing the Fe content is also significantly influencing the optical parameters of the films, a large shift of the absorption edge from 388 nm to 515 nm when  $x$  changed from 0 to 0.55. The transmittance data showed that the threshold  $\alpha$  of the fundamental absorption of the  $\text{Ti}_{1-x}\text{Fe}_x\text{O}_2$  films could be described by the expression:  $\alpha = A(E - E_g)^2$ , where  $A$  is a constant,  $E$  and  $E_g$  are the optical band gap of the ferromagnetic film and pure anatase  $\text{TiO}_2$ , respectively. The value of the exponent is characteristic for the indirect allowed transition dominating over the optical absorption [5].

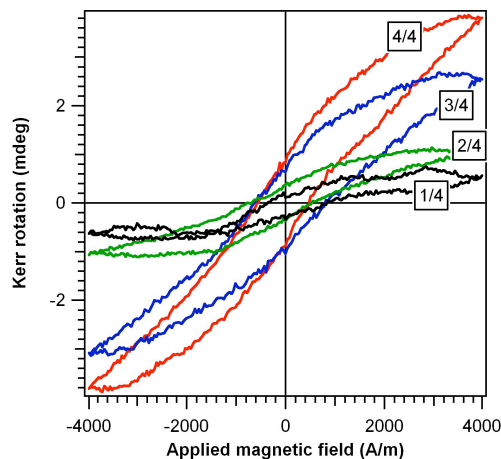


Figure 6: The MOKE loops of the investigated films.

## 4 CONCLUSION

$\text{Ti}_{1-x}\text{Fe}_x\text{O}_2$  films with  $x$  ranging between 0 and 0.55 have been fabricated by RF magnetron sputtering. The films have been characterized in terms of elemental composition, chemical state and local reactivity. The XPS and XANES results showed that, unlike the Ti case, a non-reacted  $\text{Fe}^0$  component, possibly spread in the amorphous matrix, occurs in the low-content iron samples. This component becomes less important upon increasing the values of  $x$ . This is accompanied by a red shift of the absorption edge of approximately 127 nm and a decrease of the band gap from 3.27 to 2.21 eV, under the same change in Fe composition. Preliminary (MOKE) magnetic measurements show a monotonous increase in magnetization when increasing  $x$ , while no MOKE signal could be detected in intrinsic titania films.

## ACKNOWLEDGEMENTS

The financial support from the Romanian Ministry of Education and Research through Grant 71-63/2007 MA-MAINCOPE is acknowledged. The support from Dr. A. M. Vlaicu from NIMP Bucharest for XRD measurements and from Dr. D. Zajac from HASYLAB Hamburg for XAFS measurements are greatly appreciated.

## REFERENCES

- [1] T. L. Thompson, J. T. Yates Jr., Chem. Rev. 106, 4428, 2006.
- [2] D. Luca, C. M. Teodorescu, R. Apetrei, D. Macovei, D. Mardare, Thin Solid Films, 515, 8605, 2007.
- [3] K. Seki, M. Tachiya, J. Phys. Chem. B 108, 4806, 2004.
- [4] D. Luca, D. Mardare, F. Iacomi, C.M. Teodorescu, Appl. Surf. Sci. 252, 6122, 2006
- [5] J. Tauc, *Optical Properties of Solids*, North-Holland, Amsterdam, p. 303.
- [6] D. Mardare, V. Nica, C.M. Teodorescu, D. Macovei, Surf. Sci. 601, 4479, 2007.
- [7] D. Luca, D. Macovei, C.M. Teodorescu, Surf. Sci. 600, 4342, 2006.
- [8] C.M. Teodorescu, A. El Afif, J.M. Esteva, R.C. Karnatak, Phys. Rev. B 63, 233106, 2001.
- [9] C.M. Teodorescu, J.M. Esteva, M. Womes, A. El Afif, R.C. Karnatak, A.M. Flank, P. Lagarde, J. El. Spectrosc. Relat. Phenom. 106, 233, 2000.
- [10] C.M. Teodorescu, F. Chevrier, R. Brochier, C. Richter, V. Ilakovac, O. Heckmann, P. De Padova, K. Hricovini, Eur. Phys. J. B 28, 305, 2002.
- [11] C.M. Teodorescu, D. Luca, Surf. Sci. 600, 4200, 2006.
- [12] B.K. Teo, *EXAFS: Basic Principles and Data Analysis*, Springer, Berlin, 1983.